LBNL-39325
UC-414

ERNEST ORLANDO LAWRENCE
BERKELEY NATIONAL LABORATORY

Gamma-Gamma Collider Based on Compton Back-Scattering

K.-J. Kim
Accelerator and Fusion Research Division

August 1996
Presented at the
18th International Free Electron Laser Conference,
Rome, Italy,
August 26–31, 1996,
and to be published in
the Proceedings

LOAN COPY
Circulates
for 4 weeks
Bldg. 50 Library.
Copy 2
LBNL-39325

LBNL-39325
CBP Note-196
UC-414

Gamma-Gamma Collider Based on Compton Back-Scattering*

Kwang-Je Kim
for the Gamma-Gamma Working Group**

Ernest Orlando Lawrence Berkeley National Laboratory
Berkeley, CA 94720 USA

August 1996

*This work was supported by the Office of Energy Research, Office of High Energy and Nuclear Physics, Division of High Energy Physics, of the U.S. Department of Energy under Contract No. DE-AC03-76SF00098.
**V. Telnov (BINP); T. Takahashi (Hiroshima University); S. Chattopadhyay, W. Fawley, K.-J. Kim, H. Murayama, M. Ronan, A. Sessler, M. Xie, S. Zholents (LBNL); T. Houck, D. Klem, M. Perry, K. van Bibber, G. Westenskow (LLNL); P. Chen, D. Helm, J. Irwin, J. Spencer, A. Weidemann (SLAC); and D. Meyerhofer (University of Rochester).

1. Introduction

In order to maximize accessible high energy physics, it is sensible that a future linear collider, if built, should be provided with at least two interaction regions (IRs): one for "normal" e^+e^- collisions and a second one for $\gamma\gamma$ and γe^- collisions. High energy γ- photons for these collisions are most effectively produced via Compton backscattering of focussed laser beams [1] by the high energy electron beams of the linear collider. The high energy photon beams are then brought into collision with opposing photon and electron beam for $\gamma\gamma$ collisions and γe^- collisions, respectively. The interaction region for a $\gamma\gamma$ collider therefore consists of two conversion points (CPs) where the Compton conversion occurs, and the interaction point (IP) where the collisions of $\gamma\gamma$ occur. Since positrons are not necessary for this operation, the collider may be operated in the e^-e^- mode. With suitable laser and electron beam parameters, a luminosity of $\gamma\gamma$ or γe^- collisions comparable to the of the $e^+ e^-$ collisions can be achieved. The polarization of the high energy photons can be controlled by the polarizations of the laser and the electron beam. With high luminosity and variable polarization, the $\gamma\gamma$ and γe^- collisions at TeV energies will significantly enhance the discovery potential and analytic power of a TeV linear collider complex.

An overview of a linear collider, with a second interaction region devoted to $\gamma\gamma$ collisions, is shown in Figure 1. The general scheme for the $\gamma\gamma$ interaction region is shown in Figure 2.

The concept of $\gamma\gamma$ colliders has been developed mainly by scientists from Novosibirsk, a review of which can be found in the proceedings of a recent workshop at Berkeley [2]. More serious work on the feasibility of such a collider is now under way in connection with the Next Linear Collider (NLC) design effort at Stanford Linear Accelerator Center (SLAC) [3]. In this paper we briefly review the concept, the current status, and various issues associated with the development of $\gamma\gamma$ and γe^- colliders.

A $\gamma\gamma$ collider would extend and complement the physics capability of a linear collider. For example, it is uniquely suited for direct measurement of the partial decay width of a Higgs boson

into two gamma quanta [4]. The Feynman diagram for this process involves loops of any charged particles whose mass is derived from the Higgs mechanism. A measurement of the two-photon width could help to distinguish various models predicting higher mass particles without producing them directly in accelerators.

2. Choice of Laser Parameters

The energy of the Compton backscattered photon by an intense laser field, taking into account of the electron recoil, is given by [5]

$$\hbar\omega_\gamma = \frac{x}{1+x+K^2} E_e \ , \tag{1}$$

where ω_γ is the frequency of the γ-photon, $x = 4E_e\hbar\omega_L/(mc^2)^2$, E_e = electron energy, ω_L = the frequency of the laser photon, m = electron mass, c = speed of light, and $K = e\mathscr{E}/\omega_L mc$ where $\mathscr{E}$ is the laser electric field. As $x \to 0$, eq. (1) reduces to the familiar expression for the undulator radiation in the intense laser field, with K the deflection parameter. In practical units,

$$x = 12.3\, E_e[\mathrm{TeV}]/\lambda_L[\mu\mathrm{m}] \ , \tag{2}$$

$$K^2 = 0.36\, I\left[10^{18}\mathrm{W/cm^2}\right]\lambda_L^2[\mu\mathrm{m}] \ . \tag{3}$$

Here λ_L is the laser wavelength and I is the laser intensity. Assuming $K^2 << 1$, the value of x should be smaller than 4.83; otherwise the high energy gamma photons produced by the Compton backscattering have a good chance of disappearing by colliding with other laser photons producing e^+e^- pairs (the Breit-Wheeler process) [6]. On the other hand, the maximum energy of the back-scattered gamma photon is $(x/(1+x))E_e$. For a gamma-gamma collider, x is therefore chosen to be about 4.8 in order to produce gamma photons with as high as energy as possible while avoiding the pair-production threshold. It then follows that the maximum photon energy is about 80% of the electron energy, and that the optimum laser wavelength for E_e=250 GeV is about 1 micron.

The cross section for the Compton process σ_c ranges from the classical Thomson cross section $(8/3)\pi r_0^2$ for x much smaller than unity, where r_0 is the classical electron radius, to about $\pi r_0^2 = 2.5 \times 10^{-25}\,\mathrm{cm}^2$ at x = 4.8. To produce one gamma photon per electron, the laser photons, each with an effective cross section σ_c, must cover the full transverse area of the laser pulse Σ; $\sigma_c N_{laser} \approx \Sigma$, where N_{laser} is the total number of laser photons in the pulse. On the other hand, $\Sigma \approx \lambda \ell$ because of diffraction, where ℓ is the effective length of the laser pulse, which in turn is about the same as the electron pulse length. Taking the pulse length to be about 1 ps, and using the laser wavelength of 1 μ and the Compton cross section discussed above, it follows that the $N_{laser} = 10^{19}$. This corresponds to the pulse energy of about 1J. Therefore, the requirements for generating one γ-photon per electron are a pulse energy of about 1J, peak power of about 1 TW, and intensity of about $10^{18}\,\mathrm{W/cm^2}$.

Taking into account the decrease of the available electrons as the laser beam passes by the electron beams, and neglecting the change of the laser profile seen by different electrons, the conversion efficiency is given by $k_c = 1 - \exp(-A/A_0)$, where A is the laser pulse energy and A_0 is the laser pulse energy giving rise to a conversion probability of 65%. Since the increase in the conversion probability with a laser pulse energy larger than A_0 is small, and since the laser power is expensive, one would normally choose $A = A_0$ and $k_c = 0.65$. A more accurate formula of the conversion efficiency can be found in ref. [7].

The energy of the Compton-scattered γ-photons is correlated with the backscattering angle, decreasing as the angle becomes larger. Most of the scattered photons are within an angle of about $1/\gamma$. By properly choosing the helicities of the incoming beams, the spectrum of the scattered photons can be made to have a sharp peak: the behavior of the differential Compton scattering as a function of y (= the energy of the backscattered gamma-photon/E_e) depends sensitively on the initial helicity state. When the helicity of the electrons is opposite to that of the laser photons, the differential cross section is sharply peaked in the narrow region around the maximum value of y. The peak is less prominent for the unpolarized case, and disappears

altogether when the helicities are parallel. For a gamma-gamma collider, it is clearly most advantageous to choose the first case.

3. Luminosity Optimization

The luminosity spectrum as a function of the invariant mass of the colliding γ's, the spectral luminosity, depends strongly on the distance b between the CP and the IP. Introducing the parameter $\rho = b/\gamma\sigma_y^*$, where σ_y^* is the vertical rms electron beam size (assumed to be smaller than the horizontal size) when the electrons do not experience the Compton scattering, the spectral luminosity is broadly distributed as a function of the C.M. energy in the absence of the two photon system when $\rho << 1$. As ρ is increased, the low energy part of the luminosity spectrum becomes suppressed because of the larger spot size occupied by low energy photons. Thus the luminosity spectrum develops a well defined peak at the high energy end with a bandwidth of about 20% when $\rho \simeq 1$. For most applications, one would choose $\rho \simeq 1$ to obtain a narrow spectrum without incurring a large luminosity reduction.

It turns out that the partial luminosity contained in the high energy peak (with about 20% bandwidth), $L_{\gamma\gamma}$ (peak), accounts for about $k_M = 25\%$ of the total luminosity. Therefore

$$L_{\gamma\gamma}(\text{peak}) \approx k_c^2 k_M \, L_{geom} \approx 0.1 \, L_{geom} \; . \tag{4}$$

Here L_{geom} is the geometric ee luminosity, i.e., that corresponding to the case where the electron beams are allowed to proceed to the IP and collide geometrically without the electromagnetic disruption effects, and given by

$$L_{geom} = \frac{N_e^2 f}{4\pi\sigma_x^*\sigma_y^*} \; . \tag{5}$$

Here N_e = number of electrons per bunch, f = bunch repetition frequency, and σ_x^* and σ_y^* are respectively the horizontal and vertical electron beam sizes at the IP. The luminosity of e^+e^- collisions is limited by various classical and quantum electromagnetic effects, such as beamstrahlung, disruption, pair creation, etc. As these effects are either absent or negligible in $\gamma\gamma$

collisions, a larger $L_{\gamma\gamma}$ can be achieved by producing electron beams corresponding to a larger L_{geom}. Thus, increasing N_e with a proportionate decrease in f would result in a higher luminosity while at the same time reducing the electron beam power. The beam sizes σ_x^* and σ_y^* could be reduced to a value consistent with the Oide limit [8] by either reducing the emittances or by reducing the focussing β^* value. (However, β^* should be larger than the rms bunch length.) Finally the aspect ratio $R = \sigma_x^*/\sigma_y^*$, which should be large in the e^+e^- collisions to reduce the beamstrahlung effect, can be reduced significantly.

When the CP and the IP are separated it is possible to introduce a magnet, called the "sweeping magnet," between them so that the electron-beam after the scattering could be removed from the IP. Removing the "spent" electron beam may be important in suppressing the γe and ee background events. Reducing R and thus making σ_y^* larger lessens the requirement on the field strength of the sweeping magnet, and therefore makes the construction of a sweeping magnet easier.

4. An Example for a Gamma-Gamma Collider as a Second Interaction Region for the Next Linear Collider

We now discuss a specific example for a design of a gamma-gamma collider as a second interaction region of the Next Linear Collider (NLC) at SLAC [3]. This is in a sense a minimal design, because the electron beam parameters before the final focus system are those optimized for the e^+e^- collisions rather than for the $\gamma\gamma$ collisions.

Table 1 shows the main parameters of a $\gamma\gamma$ collider as the second interaction region of the NLC. The electron beam parameters up to the final focus system are taken to be the same as that for the first interaction region (for e^+e^- collisions). However, the final focus system is modified so that the beta functions in the horizontal and the vertical directions become the same values, 0.5 mm. This leads to a geometric electron-electron luminosity (again assuming the electrons are allowed to collide without being Compton scattered) of about $1 \times 10^{34}/\text{cm}^2/\text{s}$, which is about

twice that of the e^+e^- collisions. The $\gamma\gamma$ luminosity within 20% of the high energy peak is about $1 \times 10^{33}/cm^2/s$.

5. Laser Path in IR

A possible mirror arrangement to bring the laser pulses to the conversion point and to dispose of them in the tight space limited by the vertex chamber, the mask, and quadrupoles is shown in Fig. 3 [9]. The figure shows the inner radius of the vertex chamber surrounding the CP and the IP (the separation between these points is not resolved in the scale of this figure), and its neighborhood, including the quadrupole holders closest to the IP. The straight line and the narrow cone passing through the quadrupole holder are, respectively, the incoming and the disrupted electron beam. The small elliptical objects are the mirrors, the numbers indicating the sequence of the laser beam deflections. The laser beam, indicated by thin cylinders, enters from below the quadrupole holder on the right hand side, deflected by mirrors 1 to 5, and focussed to the CP by mirror 6. Although mirror 6 has a small hole for the incoming and outgoing electron beams, the loss is small because of its large diameter (~60 cm). After the focus, the laser beam proceeds to the left hand side of the chamber, and reflected by mirror 11 and is focussed to the second CP. It then is transported back to the right hand, and exits the chamber. The quarter wave plate between mirror 10 and 11 is for the polarization control. Using only spherical surfaces, the optics can be designed for a Strehl ratio higher than 0.9.

A single laser pulse is used twice in this scheme so that the requirement on the average laser power can be reduced compared to the single pass scheme. Due to the fact that the separation between two CP transits are about 10 times larger than the electron bunch spacing, and also due to the loss on mirrors, the reduction is estimated to be about 30% rather than 50%.

The above scheme can be refined to a four pass scheme by introducing a thin film reflector [10].

It is also possible to design the laser pulse to bounce back and forth along the same pass, thus forming a cavity mode. By building up the cavity power from low-power, externally

injected pulses, the average power requirement could be reduced by the cavity Q. A confocal cavity configuration was proposed for the $\gamma\gamma$ collider in which the end mirrors can accommodate holes for the electron beam passage without losing optical beams [11].

6. Lasers

Finally, we address the question of developing a laser for the purposes of a $\gamma\gamma$ collider. The requirements listed in Table 1 are a pulse of about 1 joule, a pulse length of a few picoseconds (corresponding to a peak power of a few terrawatts), an average power of 16 kilowatts (corresponding to about 100 bunches per pulse and a rep-rate of about 160 Hz), and variable polarization. Although the multipass approach discussed in the previous section could reduce these requirements, a $\gamma\gamma$ collider requires a laser power substantially beyond what is currently available.

One approach is the solid state laser. Using the chirped pulse amplification technique, solid-state lasers already give peak powers that satisfy the requirements [12]; they only fail our needs in that the average power is currently in the few watt range.

High power diode lasers for pumping and lasing materials that can handle high thermal loading are two major efforts on advancing diode laser technologies for high average power already under way as part of both military and civilian projects. Advanced solid state materials, either athermal glass hosts or new crystals specifically engineered for diode pumping, are also being actively developed. Based on these developments, the 16 kW laser needed for a gamma - gamma collider can in principle be built out of 1 kW unit cells [13].

Another possibility is a free-electron laser (FEL). One possible approach is a two-stage MOFA configuration consisting of an FEL oscillator driven by a 50 MeV linac and an FEL power amplifier driven by a 2 GeV linac [14]. However, it is difficult to achieve the TeV peak power in conventional FEL. The peak power is given by $P = \eta E_e I$, where η is the efficiency, E_e = electron energy, I = beam current. Taking optimistic numbers, $\eta = 10\%$ and I = 1 kA, it is necessary to have $E_e = 10$ GeV which is not matched well to a 1 μm FEL.

A more innovative approach is to import the chirped pulse amplification technique developed for solid state lasers discussed in previous section to FEL [6], that is, to use FELs to amplify chirped pulses much larger than a few pico seconds and then compress them later. Two such schemes were proposed, one based on a regenerative FEL amplifier driven by an RF linac [15], and another based on a high-gain FEL amplifier driven by an induction linac [16]. In the first scheme the electron beam consists of a sequence of 50-ps-long bunches separated by the RF period. It requires intracavity optical switches operating in a high-power environment. In the second scheme, an induction linac with 1 kA, 100 MeV electron beam is used. The input signal is contiguous chirped pulses each 1.4 ns long. The design of the induction linac producing the required electron beam is challenging but within the current state-of-the-art [17].

7. Conclusions

We have seen that a $\gamma\gamma$ collider is technically possible and that it would open up important new possibilities for particle physics research. Such a project will require a significant investment in preparatory research and development. It is hoped that the high energy community will respond to the outstanding promise of the gamma-gamma collider idea.

References

[1] F.R. Arutyunian and V.A. Tumanian, Phys. Lett. 4, 176 (1963); R.H. Milburn, Phys. Rev. Lett. 10, 75 (1963).
[2] Proc. of Workshop on Gamma-Gamma Colliders, Berkeley CA, USA, 1994; Nucl. Instr. Methods A 355, 1–194 (1995); A Second Interaction Region for Gamma-Gamma, Gamma-Electron and Electron-Electron Collisions for NLC, LBNL-38985, LLNL-UCRL-ID-124181, SLAC-PUB-95-7192.
[3] Zeroth-Order Design Report for the Next Linear Collider, Appendix B, LBNL-PUB-5424, SLAC Report 474, UCRL-ID-124161 (May 1966.
[4] J.F. Gunion, J.G. Kelly, J. Ohnemus, Phys. Rev. D51, 2101 (1995).
[5] See for a review, V.B. Berestetskii, E.M. Lifshitz, L.P. Pitaevskii, Quantum Electrodynamics, Section 101 (Pergamon Press 1982).
[6] V. Telnov, Proc. of Workshop on Gamma-Gamma Colliders, Berkeley CA, USA, (1994); Nucl. Instr. Methods A 355 (1995).
[7] Reference [2], Section B.6.3.
[8] K. Oide, Phys. Rev. Lett., 61 (1988) 1713.
[9] D. Klem and L. Seppala, to be published.

[10] D. Klem, private communications.
[11] M. Xie, Reference [2], Section B.8.4.
[12] For a review, see M.D. Perry and G. Mourou, Science, 264 (1994) 917.
[13] D. Meyerhofer and M.D. Perry, Ref [2] Section B.11.
[14] E.L. Saldin, V.P. Sarantsev, E.A. Schneidmiller and M.V. Yurkov, Nucl. Instr. Methods A 355 (1995) 171.
[15] K.C.D. Chan, J.C. Goldstein, D.C. Nguyen, and H. Takeda, Proceedings of 1995 Particle Accelerator Conference, page 228.
[16] K.-J. Kim, M. Xie, and A. Sessler, NIM, A375 (1996) 523.
[17] T. Houck and G. Westenskow, Ref. [2], Section B.12.3.

Figure Captions

Fig. 1. A Linear Collider with a second interaction region devoted to γ-γ collisions.
Fig. 2. General schematic of a $\gamma\gamma$ collider interaction point.
Fig. 3. Mirror arrangement in $\gamma\gamma$ interaction region.

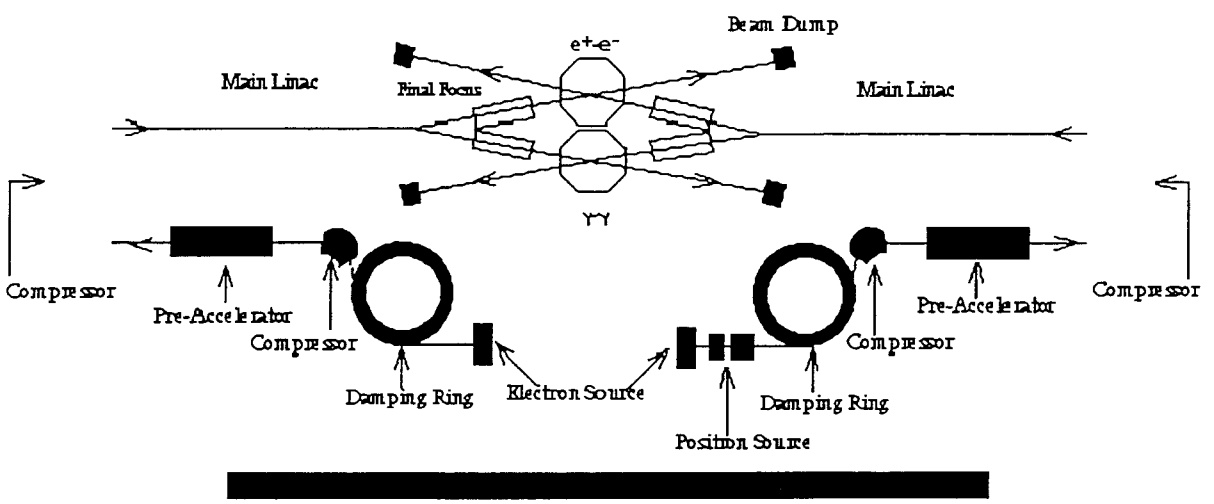

Fig. 1

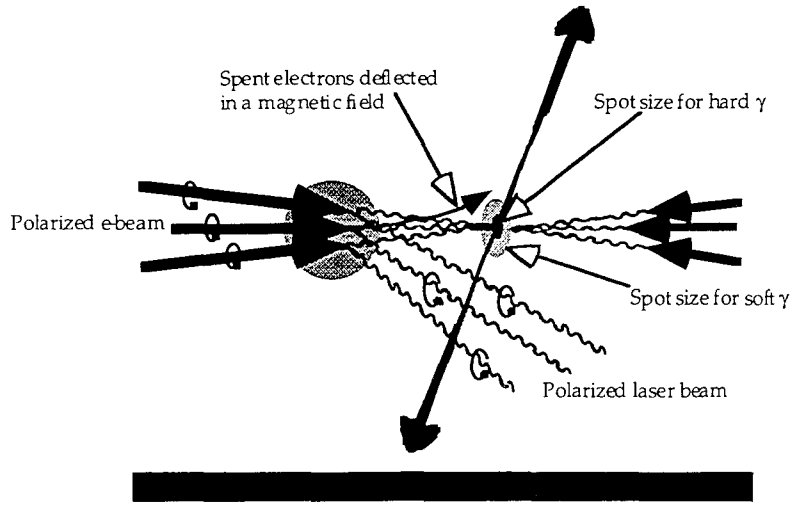
Spent electrons deflected
in a magnetic field
Spot size for hard γ
Polarized e-beam
Spot size for soft γ
Polarized laser beam

Fig. 2

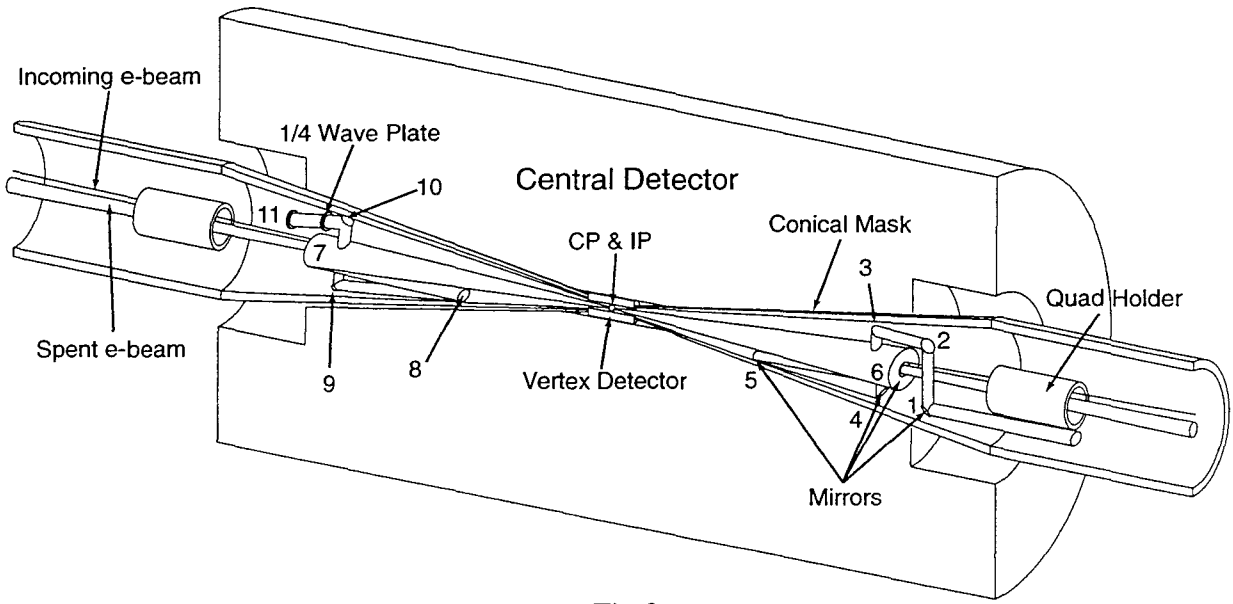
Incoming e-beam
1/4 Wave Plate
Central Detector
10
11
7
CP & IP
Conical Mask
3
Quad Holder
Spent e-beam
2
9
8
Vertex Detector
5
6
1
4
Mirrors

Fig 3

Table 1. Electron and laser parameters for $\gamma\gamma$ interaction region at the NLC.

Electron Beam parameters:

Electron energy	250 GeV
Repetition rate	90 bunches separated by 1.4 ns, 180 Hz
Particles per bunch	$N_e = 0.65 \times 10^{10}$
Normalized rms emittance	$\gamma\varepsilon_x = 5 \times 10^{-6}$ m-r, $\gamma\varepsilon_y = 8 \times 10^{-8}$ m-r
Beta function at the IP	$\beta_x^* = \beta_y^* = 0.5\,\mathrm{mm}$
Rms bunch length	$\sigma_z = 0.1$ mm
Polarization	Fully polarized with helicity switching capability
CP-IP distance	b = 5 mm

Laser Beam parameters:

Wavelength	$\lambda = 1.053$ μm
Micropulse energy	A = 1 J
Rayleigh length	$Z_R = 0.1$ mm
Rms micropulse length	$\sigma_{Lz} = 0.23$ mm
Peak intensity	1×10^{18} W/cm
Average power	16.2 kW per conversion
Polarization	Fully polarized with helicity switching capability

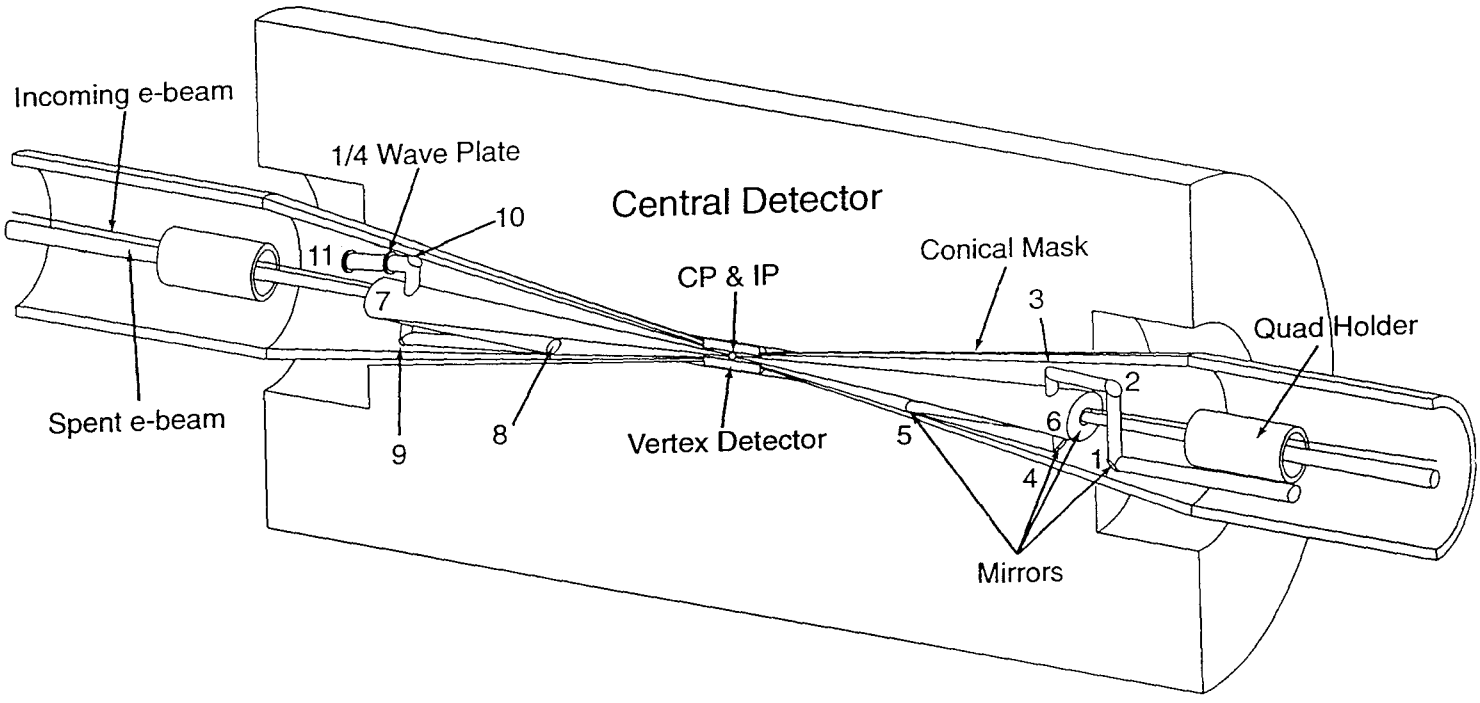
Incoming e-beam
1/4 Wave Plate
Central Detector
10
11
7
CP & IP
Conical Mask
3
Quad Holder
2
Spent e-beam
9
8
Vertex Detector
5
6
1
4
Mirrors